ChemComm

Perylenediimide promoted charge transfer in tetracyanobutadiene-triphenylamine (TCBD-TPA) and expanded-tetracyanobutadiene-triphenylamine (DCNQ-TPA) push-pull conjugates

Journal:	*ChemComm*
Manuscript ID	CC-COM-01-2025-000578.R1
Article Type:	Communication

ChemComm

COMMUNICATION

Perylenediimide promoted charge transfer in tetracyano butadiene-triphenylamine (TCBD-TPA) and expanded-tetracyano butadiene-triphenylamine (DCNQ-TPA) push-pull conjugates

Received 00th January 20xx,
Accepted 00th January 20xx

DOI: 10.1039/x0xx00000x

Mohd Wazid,[a] Yogajivan Rout,[a] Ajyal Z. Alsaleh,[b] Ram R. Kaswan,[c] Rajneesh Misra,[a*] and Francis D'Souza[c*]

The significance of perylenediimide (PDI) in promoting excited charge transfer in push-pull systems carrying TCBD-TPA and DCNQ-TPA, synthesised via Pd(II)-catalysed Sonogashira cross-coupling reaction followed by [2+2] cycloaddition retroelectrocyclization (CA–RE) reaction, is demonstrated using femtosecond transient absorption and other pertinent methods.

Push-pull chromophores find widespread applications in organic electronics, dye lasers, optical power limiters, solar energy harvesting, fluorescence sensing, and bio-probing.[1–4] The π-conjugated perylenediimides have attracted considerable interest due to their unique characteristics, including strong intramolecular charge transfer, good photochemical and thermal stability, low cost, flexibility, and light weight, making them a sought-after material for organic electronic applications.[5–10] Additional features of PDIs are strong optical absorption in the visible region, high extinction coefficient, good electron acceptor capabilities, stabilised low-lying LUMO energy levels, and ease of functionalisation at the -*ortho, -imide,* and *bay* positions.[11]

The push-pull strength and its properties can be manipulated by adjusting the strength of donor and acceptor subunits or modifying the rigid backbone structure of the D-A chromophores.[12] The thermal, photophysical, and electrochemical properties of push-pull chromophores can be tailored by incorporating strong electron acceptors, such as TCBD and DCNQ, via [2+2] cycloaddition-retroelectrocyclization (CA–RE) reaction.[13-15] This is crucial in understanding how the photosensitizer PDI modulates the charge transfer ability when coupled to TCBD/DCNQ. Herein, we have undertaken this task and report PDI-TCBD/DCNQ-D (D = donor = triphenylamine, TPA), whose structures and control compounds are shown in Scheme 1. The extended π–conjugation is expected to improve the interaction between the donor and acceptor units within the push-pull systems, and the strong electron-accepting groups (TCNE and TCNQ) at the *bay* side of the TPA-substituted PDI chromophores are expected to allow efficient transfer and stabilise separated states in polar solvents.

Scheme 1 below outlines the developed synthetic strategy. The precursors 1-ethynyl-4-(phenylethynyl) benzene (1), 4-((4-ethynylphenyl) ethynyl)-N,N-diphenylaniline (2), and Br-PDI were synthesised by the reported procedure.[16] The acetylene bridge derivatives PDI-Ph_2 and PDI-TPA were synthesised using a Palladium-catalyzed Sonogashira cross-coupling reaction between Br-PDI and precursors (1) and (2). The reactions were carried out in a 1:1 mixture of toluene and diisopropylamine at 80 °C, resulting in PDI-Ph_2 and PDI-TPA in 74% and 83% yields, respectively. The PDI-TCBD-TPA was synthesised via [2+2] CA–RE reaction, where PDI-TPA was reacted with 2.0 equivalents of TCNE in dichloroethane (DCE) at 120 °C, resulting in PDI-TCBD-TPA in 72% yield. Similarly, PDI-TPA was reacted with 2.0 equivalents of TCNQ in dichloroethane (DCE) at 120 °C, resulting in DCNQ-bridged compound PDI-DCNQ-TPA in 80% yield. These compounds were found to be soluble in common organic solvents, such as toluene, dichloromethane, tetrahydrofuran, dimethylformamide, and chloroform, and are well-characterised by ^{1}H NMR, ^{13}C NMR, and MALDI techniques (Figs. S1–S12 in ESI).

Fig. 1a shows the absorption spectra of the investigated compounds in DCB. PDI-Ph_2 revealed the typical spectrum of PDI with prominent peaks at 450, 500, and 545 nm due to π-π* transition with vibronic fine structure. These peaks are red-shifted by about 25 nm compared to pristine PDI, revealing the effect of extended π–conjugation. Replacing the terminal phenyl entity with a TPA entity in PDI-TPA caused significant spectral broadening. The prominent peak corresponding to TPA was observed at 380 nm. In the case of PDI-TCBD-TPA and PDI-DCNQ-TPA, the fine vibrational structures of PDI could be restored; however, the peak corresponding to TPA at 380 nm revealed diminished intensity due to CT interactions involving the directly connected TCBD/DCNQ entities. A new broad peak spanning 570–900 nm was observed in the case of PDI-DCNQ-

[a] *Department of Chemistry, Indian Institute of Technology (IIT-I), Indore 453552, India. E-mail: rajneeshmisra@iiti.ac.in*
[b] *Chemistry Department, Science College, Imam Abdulrahman bin Faisal University, Dammam 34212, Saudi Arabia*
[c] *Department of Chemistry, University of North Texas, 1155 Union Circle, #305070, Denton, TX 76203-5017, USA, E-mail: Francis.DSouza@UNT.edu.*
Supplementary Information available: Synthesis and Experimental details, additional fs-TA and ns-TA spectral data. See DOI: 10.1039/x0xx00000x

TPA. This peak had charge transfer (CT) characteristics due to the interaction between the electron-deficient DCNQ and electron-rich TPA.[12,15]

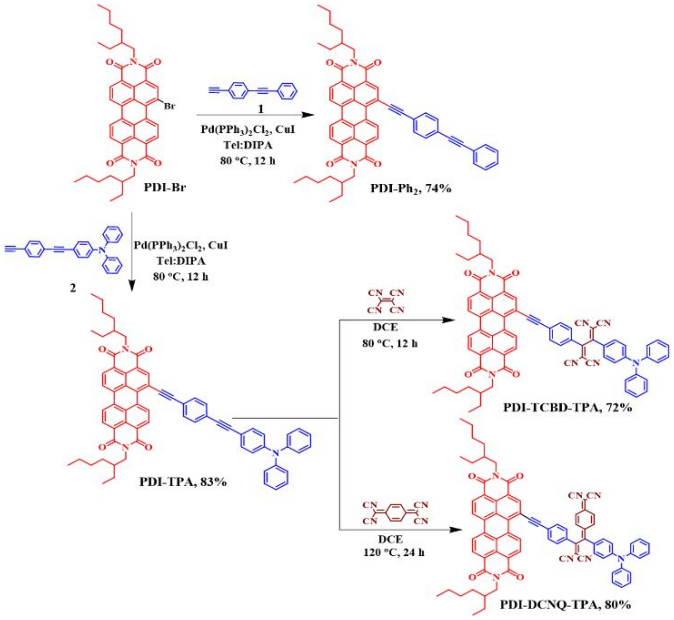

Scheme 1 Synthesis of PDI-TCBD/DCNQ-D and the control compounds.

Fig. 1b shows the fluorescence spectrum of the investigated compounds. PDI-Ph_2 revealed a broad emission centred at 575 nm. PDI-TPA revealed quenched emission (>94%) but was highly redshifted at 664 nm, consistent with the previously discussed charge transfer origin. The PDI emission in PDI-TCBD-TPA and PDI-DCNQ-TPA was substantially quenched (>97%), suggesting its involvement with the attached TCBD-TPA and DCNQ-TPA entities in the excited state.

Subsequently, electrochemical studies using both cyclic voltammetry (CV) and differential pulse voltammetry (DPV) were performed to evaluate the redox potential and the level of redox modulation caused by the D and TCBD/DCNQ entities (See Fig. S13 and Table S1). The oxidation and first reduction of PDI-Ph_2 were located at 1.73 and –0.48 V vs. Ag/AgCl in dichlorobenzene (DCB) containing 0.1 M (TBA)ClO_4. The introduction of TPA in PDI-TPA

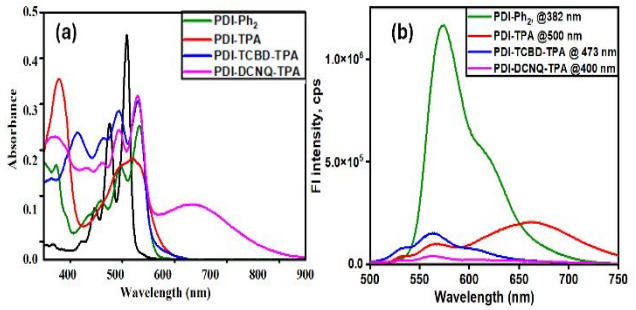

Fig. 1. (a) Absorption spectra of the indicated compounds in DCB (conc. = 1 x 10^{-5} M). (b) The fluorescence spectrum of the indicated compounds at the excitation wavelengths is shown. (The fluorescence intensity (FI) of PDI-Ph_2 was adjusted by multiplying the original value by 0.3)

revealed an additional oxidation peak at 1.10 V due to TPA oxidation; while the PDI reduction did not show significant changes, PDI oxidation was anodically shifted by 50 mV and appeared at 1.69 V. The reductions of TCBD in PDI-TCBD-TPA appeared at –0.20 and –0.61 V, while the PDI-centred reductions were at –0.48 and –0.71V. Facile reduction of TCBD over PDI in this compound was apparent. On the oxidation side, TPA oxidation was anodically shifted and appeared at 1.39 V due to the electronically induced effects caused by the neighbouring TCBD. The PDI-centred oxidation also exhibited an anodic shift, appearing at 1.78 V. Replacing TCBD with DCNQ in PDI-DCNQ-TPA revealed DCNQ-centred reduction at –0.29 and –0.30 V. In contrast, PDI reductions did not experience appreciable changes. TPA oxidation at 1.11 and PDI oxidation at 1.74 V were also noted. The facile reduction of DCNQ over TCBD and the redox modulation of other entities were borne out of this study.

Subsequently, DFT and TD-DFT studies using CAM-B3LYP/6-31G(d,p) basis set[17] were performed to visualise optimised geometry, frontier orbitals, and excited state CT (charge shift) events involving different excited states. They are summarised in Fig. 2. In all the three push-pull systems investigated here, no steric hindrance was observed, thanks to the extra phenylacetylene spacer. For PDI-TPA, HOMO on TPA and LUMO on PDI was noted. TD-DFT studies revealed a clear charge shift (difference in charge between the ground and the excited states) from $S_0 \rightarrow S_2$ and $S_0 \rightarrow S_3$ states (the involved orbital contributions, calculated wavelength, and oscillator strength of the transition are listed below each figure). In the case of PDI-TCBD-TPA, the majority HOMO on TPA and LUMO on PDI-TCBD entity was observed. Clear CT transitions were observed from the S0→S2 and S0→S3 states, involving terminal TPA to TCBD and PDI-TCBD. Similarly, in the case of PDI-DCNQ-TPA, HOMO on the DCNQ-TPA and LUMO on PDI-TCBD were observed (the HOMO–1 was solely on the PDI entity). CT events were observed from the $S_0 \rightarrow S_1$ and $S_0 \rightarrow S_3$ states wherein TPA losing electron (donor) and DCNQ and PDI-DCNQ accepting electron was borne out from this exercise (see Fig. S14–S21 for additional results). This study effectively summarises the role of each entity in excited-state events.

Jablonski diagrams constructed using free energy calculations[15a,18] help understand different photochemical events. As shown in Fig. 3, such a diagram has been built for PDI-TCBD-TPA and PDI-DCNQ-TPA. In both push-pull systems, selective excitation of PDI would generate ^{1}PDI* that would undergo initial CT to yield $(PDI\text{-}TCBD)^{\delta-}\text{-}(TPA)^{\delta+}$ and $(PDI\text{-}DCNQ)^{\delta-}\text{-}(TPA)^{\delta+}$. The earlier discussed frontier orbitals support the involvement of both PDI/TCBD or PDI/DCNQ in the initial CT formation, as shown in Fig. 3. In a polar solvent such as benzonitrile, the CT state undergoing the charge separation (CS) state is energetically feasible. Such a CS process would yield $(PDI\text{-}TCBD)^{\cdot-}\text{-}(TPA)^{+\cdot}$ and $(PDI\text{-}DCNQ)^{\cdot-}\text{-}(TPA)^{+\cdot}$ radical ion pairs. The calculated energy of the $(PDI\text{-}TCBD)^{\cdot-}\text{-}(TPA)^{+\cdot}$ is above that of the ^{3}PDI* (~1.07 eV), and under such conditions, the CS state could relax to the ^{3}PDI* state before returning to the ground state. In contrast, the energy of the $(PDI\text{-}DCNQ)^{\cdot-}\text{-}(TPA)^{+\cdot}$ state is much below that of ^{3}PDI*, which would prompt the CS state

to relax directly to the ground state. Pump-probe studies were performed to verify these photochemical paths to derive structure-dynamics properties.

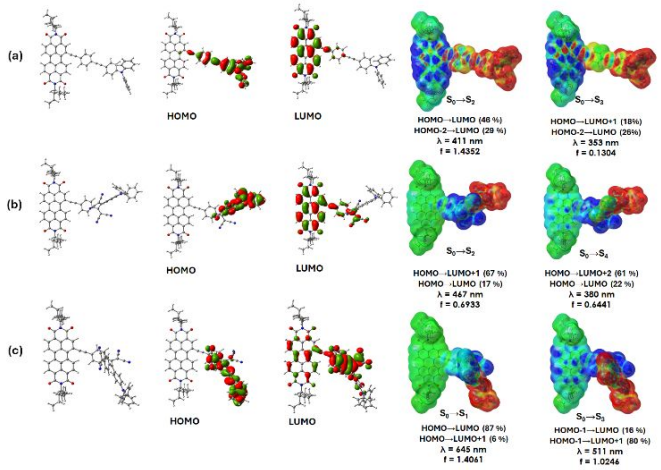

Fig. 2 Optimized geometry, frontier orbitals, and excited state CT (charge shift) events from different excited states for a) PDI-TPA, b) PDI-TCBD-TPA, and c) PDI-DCNQ-TPA at the CAM-B3LYP/6-31G(d,p) SCRF (CPCM, solvent = benzonitrile) level.

The fluorescence lifetime of PDI-Ph_2 was recorded and found to be 6.14 ns (in toluene, monoexponential decay; see Fig. S22 for decay curve). For other studied systems, the lifetime was much lower than the time resolution of our setup (~200 ps).

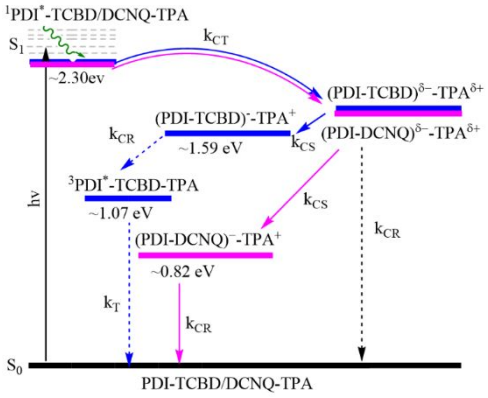

Fig. 3 Jablonski diagram depicting different photo events in PDI-TCBD-TPA and PDI-DCNQ-TPA push-pull systems.

Femtosecond transient absorption (fs-TA) spectra of PDI-Ph_2 in benzonitrile are shown in Fig. S23. Spectral features were typical of PDI[19] with a negative signal at 556 nm having contributions from both ground state bleach (GSB) and stimulated emission (SE). Excited state absorption (ESA) peaks were also observed at 744, 761, and 786 nm. The recovery of the GSB/SE and the decay of the ESA peaks was rather slow, consistent with the relatively longer singlet lifetime.

The fs-TA spectra of PDI-TPA are shown in Fig. 4a. The spectral features significantly differed from the control PDI-Ph_2. Broad positive absorption was observed in the 570–700 nm in addition to the expected GSB/SE and ESA peaks corresponding to ^{1}PDI*. Chemical oxidation of PDI-TPA confirmed that these features are due to CS products (see Fig S24 for spectral changes during chemical oxidation and reduction). The data was subjected to GloTarAn analysis.[20] A three-component fit was satisfactory, and decay-associated spectra (DAS) are shown in the right-hand panel (Fig. 4a, right-hand panel). The CS state persisted for about 10.7 ps (representing the average lifetime of the species; see Fig. S25 for population time profile plots).

The fs-TA spectra of PDI-TCBD-TPA are shown in Fig. 4b and provide evidence of CS. The new spectral features in the visible region agreed well with the spectrum of the chemically oxidised/reduced species (Figs. S24c and S24d). Data analysis revealed a 3-component fit to be satisfactory and resulted in a CS lifetime of 9.88 ps (see Figs. 4b for DAS and S25b for population time profiles). The situation was also similar for the PDI-DCNQ-TPA system. In this case, the spectral features overlapped with the ESA peaks, as shown in Fig. 5c (Figs. S24e and S24f for spectra of oxidised and reduced species). A three-component fit resulted in a CS lifetime of 24.11 ps (see Figs. 4c for DAS and S25c for population time profiles). In summary, fs-TA spectral studies successfully revealed CS in the three push-pull systems studied here. A comparison of the lifetimes of the CS states of PDI-TCBD-TPA and PDI-DCNQ-TPA deserves some discussion. A ~10 ps in the former and ~24 ps in the latter suggest faster recombination in the former case, which could be rationalised based on the intermediate population of ^{3}PDI*

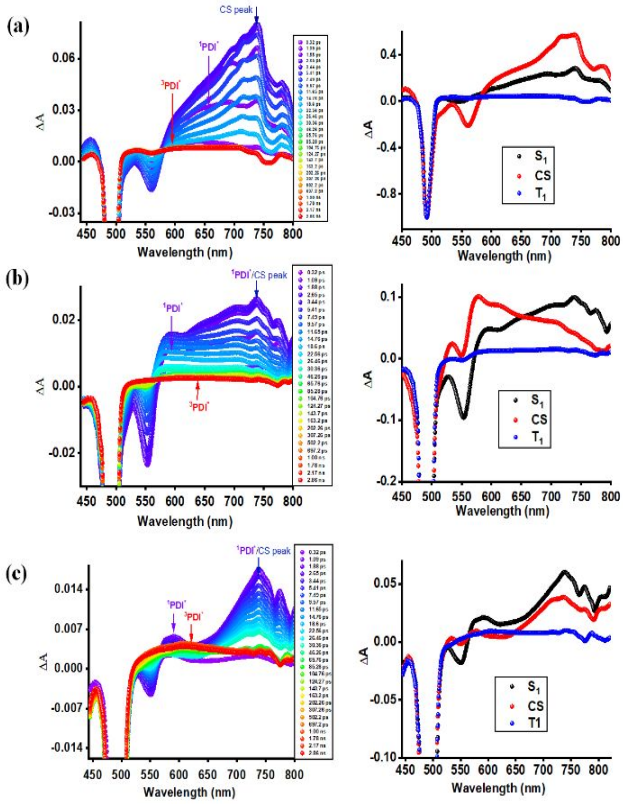

Fig. 4 Fs-TA spectra at the indicated delay times of (a) PDI-TPA, (b) PDI-TCBD-TPA, and (c) PDI-DCNQ-TPA push-pull systems in benzonitrile (λ_{ex} = 499 nm). The DAS is shown on the right-hand side.

in the latter case (see Fig. 3 blue path), while in the former case, the CS state relaxes directly to the ground state (see Fig. 3 magenta path). These observations highlight the significance of intermediate triplet states in modulating the dynamics of the CS process.

In summary, the newly synthesised and studied push-pull systems, PDI-TPA, PDI-TCBD-TPA, and PDI-DCNQ-TPA, revealed several important observations. While PDI-TPA acted as a simple donor-acceptor system revealing CT emission, incorporating TCBD and DCNQ improved the overall electron-acceptor property of PDI-TCBD and PDI-DCNQ entities while modulating the redox potentials. TD-DFT studies revealed the contributions of different excited states in promoting initial charge transfer following the charge separation. Fs-TA studies in polar benzonitrile provided evidence of charge separation and the relative positioning of the CS state with respect to the triplet state of PDI, which governs the final lifetimes of the CS states. Further studies in this area are currently underway in our laboratories.

We acknowledge the support of the US National Science Foundation (2345836 to FD), the Council of Scientific and Industrial Research (Project No. 01/3112/23/EMR-II), and Science and Engineering Research Board (SERB) projects CRG/2022/000023 and STR/2022/000001, New Delhi. We are grateful to the DST-FIST grant for the 500 MHz NMR facility and the Sophisticated Instrumentation Centre (SIC) at IIT-I. M.W. thanks IIT-I for a fellowship.

Data availability

The data supporting this article have been included as part of the ESI.

Conflict of interest

There are no conflicts to declare.

Notes and references

1 T. Michinobu, C. Boudon, J. Gisselbrecht, P. Seiler, B. Frank, N. N. P. Moonen, M. Gross and F. Diederich, *Chem. Eur. J.*, 2006, **12**, 1889–1905.
2 J. Hankache and O. S. Wenger, *Chem. Rev.*, 2011, **111**, 5138–5178.
3 A. B. Ricks, G. C. Solomon, M. T. Colvin, A. M. Scott, K. Chen, M. A. Ratner and M. R. Wasielewski, *J. Am. Chem. Soc.*, 2010, **132**, 15427–15434.
4 T. C. Parker, D. G. (Dan) Patel, K. Moudgil, S. Barlow, C. Risko, J.-L. Brédas, J. R. Reynolds and S. R. Marder, *Mater. Horiz.*, 2015, **2**, 22–36.
5 F. Würthner, C. R. Saha-Möller, B. Fimmel, S. Ogi, P. Leowanawat and D. Schmidt, *Chem. Rev.*, 2016, **116**, 962–1052.
6 H. A. Bent, *Chem. Rev.*, 1968, **68**, 587–648.
7 W. Jiang, Y. Li and Z. Wang, *Acc. Chem. Res.*, 2014, **47**, 3135–3147.
8 O. Ostroverkhova, *Chem. Rev.*, 2016, **116**, 13279–13412.
9 D. Gutierrez-Moreno, A. Sastre-Santos and F. Fernandez-Lazaro, *Org. Chem. Front.,* 2019, **6**, 2488-2499.
10 F. Würthner, *Chem. Commun.*, 2004, 1564–1579.
11 A. Nowak-Król and F. Würthner, *Org. Chem. Front.*, 2019, **6**, 1272–1318.
12 R. Misra and S. P. Bhattacharyya, *Intramolecular Charge Transfer: Theory and Applications*, John Wiley & Sons, 2018.
13 (a) T. Michinobu and F. Diederich, *Angew. Chem., Int. Ed.*, 2018, **57**, 3552−3577; (b) M. Kivala and F. Diederich, *Acc. Chem. Res.,* 2009, **42**, 235−248.
14 (a) M. Sekita, B. Ballesteros, F. Diederich, D. M. Guldi, G. Bottari and T. Torres, *Angew. Chem., Int. Ed.*, 2016, **55**, 5560−5564: (b) K. A. Winterfeld, G. Lavarda, J. Guilleme, M. Sekita, D. M. Guldi, T. Torres and G. Bottari, *J. Am. Chem. Soc.*, 2017, **139**, 5520−5529; (c) A. Gopinath, N. Manivannan, S. Mandal, N. Mathivanan and A. S. Nasar, *J. Mater. Chem. B.*, 2019, **7**, 6010–6023; (d) A. T. Bui, C. Philippe, M. Beau, N. Richy, M. Cordier, T. Roisnel, L. Lemiegre, O. Mongin, F. Paul and Y. Trolez, *Chem. Commun.,* 2020, **56**, 3571–3574; (e) C. Philippe, A. T. Bui, M. Beau, H. Bloux, F. Riobe, O. Mongin, T. Roisnel, M. Cordier, F. P. L. Lemiegre and Y. Trolez, *Chem. Eur. J.,* 2022, **28**, e202200025; (f) Z. Pokladek, N. Ripoche, M. Betou, Y. Trolez, O. Mongin, J. O. Banska, K. Matczyszyn, M. Samoc, M. G. Humphrey, M. B. Desce and F. Paul, *Chem. Eur. J.*, 2016, **22**, 1–14; (g) P. S. Rao, S. Brixi, D. B. Shaikh, M. Al Kobaisi, B. H. Lessard, S. V. Bhosale and S. V. Bhosale, *Eur. J. Org. Chem*., 2021, 2615-2624. (h) X. Chen and T. Michinobu, J. Org. Chem. 2025, 90, 1561–1570; (i) B. Pigulski, K. Misiak, P. Męcik and S. Szafert, *Chem. Eur. J.* 2023, e202302725; (j) L. Mateo, L Sagresti, Y Luo, D M. Guldi, T Torres, G. Brancato and G. Bottari, *Chem. Eur. J*. 2021, **27**, 16049-16055.
15 (a) R. Sharma, M. B. Thomas, R. Misra and F. D'Souza, *Angew. Chem. Int. Ed.,* 2019, **58**, 4350–4355; (b) D. Pinjari, A. Z. Alsaleh, Y. Patil, R. Misra and F. D'Souza, *Angew. Chem. Int. Ed.*, 2020, **59**, 23697–23705; (c) I. S. Yadav, A. Z. Alsaleh, R. Misra and F. D'Souza, *Chem. Sci.,* 2020, **12**, 1109– 1120; (d) T. Shoji and S. Ito, *Chem. Eur. J.*, 2017, **23**, 16696–16709; (e) A. W. Dawson, B. Sekaran, S. Das, R. Misra and F. D'Souza, *J. Phys. Chem. C* 2024, **128**, 18857-18871 (f) S. Das, Y. Rout, M. Poddar, A. Z. Alsaleh, R. Misra and F. D'Souza, *Chem. Eur. J.* 2024, e202401959 (1 of 16); (g) A. Z. Alsaleh, D. Pinjari, S. Das, R. Misra and F. D'Souza, *J. Phys. Chem. C* 2024, **128**, 7188-7201; (h) I. S. Yadav, R. R. Kaswan, A. Liyanage, R. Misra and F. D'Souza, *J. Phys. Chem. C* 2024, **128**, 4934-4945; (i) P. K. Gupta, S. Das, R. Misra and F. D'Souza, *Chem. Eur. J*. 2024, e202304313 (1 of 13); (j) M. Guragain, D. Pinjari, R. Misra and F. D'Souza, *Chem. Eur. J*. 2023, **29**, e202302665 (1 of 12). (k) I. Yadav, J. K. Sharma, M. Sankar and F. D'Souza, *Chem. Eur. J.* **29**, e202301341 (1 of 8); (l) C. Popli, Y. Jang, R. Misra and F. D'Souza, *J. Phys. Chem. B* 2023, **127**, 4286-4299; (m) Y. Jang, B. Sekaran, P. P. Singh, R. Misra and F. D'Souza, *J. Phys. Chem. A* 2023, **127**, 4455-4462. (n) I. S. Yadav, A. Z. Alsaleh, B. Martin, R. Misra and F. D'Souza, *J. Phys. Chem. C* 2022, **126**, 13300-13310; (o) M. Sheokand, A. Z. Alsaleh, F. D'Souza and R. Misra, *J. Phys. Chem. B* 2023, **127**, 2761-2773; (p) I. S. Yadav, Y. Jang, Y. Rout, M. B. Thomas, R. Misra and F. D'Souza, *Chem. Eur. J.* 2022, e202200348 (1 of 13).
16 (a) T. Guner, E. Aksoy, M. M. Demir and C. Varlikli, *Dyes and Pigments*, 2019, **160**, 501–508; (b) L. Pålsson, C. Wang, A. S. Batsanov, S. M. King, A. Beeby, A. P. Monkman and M. R. Bryce, *Chem. Eur. J.*, 2010, **16**, 1470–1479.
17 *Gaussian 09*, Revision A.02, M. J, Gaussian, Inc., Wallingford, CT, USA, 2009.
18 D. Rehm and A. Weller, *Isr. J. Chem.*, 1970, **8**, 259–271.
19 A. M. Gutierrez-Vilchez, C. A. Ileperuma, V. Navarro-Perez, P. A. Karr, F. Fernandez-Lazaro and F. D'Souza, *ChemPlusChem*, 2024, **89**, e202400348 (1 of 11).
20 J. J. Snellenburg, S. Laptenok, R. Seger, K. M. Mullen and I. H. M. van Stokkum, I. H., *J. Stat. Softw.,* 2012, **49**, 1–22.

Data availability statement

The data supporting this article have been included as part of the ESI.